pH Dependence of the Active Site of Horseradish Peroxidase Compound II†

C. S. Chang,‡,§ I. Yamazaki,‡ R. Sinclair,‡ S. Khalid,‖ and L. Powers*,‡

National Center for the Design of Molecular Function, Utah State University, Logan, Utah 84322-4630, and National Synchrotron Light Source, Brookhaven National Laboratory, Building 725A X9, Upton, New York 11973

Received June 5, 1992; Revised Manuscript Received October 27, 1992

ABSTRACT: Using X-ray absorption spectroscopy, we investigated the active site of horseradish peroxidase (HRP) compound II at two different pH values. The results indicate that the bond length of the sixth coordinated ligand of the active site was 1.90 ± 0.02 Å at pH 7, decreasing to 1.72 ± 0.02 Å at pH 10. The average iron-to-pyrrole nitrogen and the proximal ligand bond lengths showed no significant changes. The position of higher coordination shells around the iron center changed, implying that some movement or deformation of nearby amino acid residues and/or of the heme occurred. Results of this study suggest that the decrease of the Fe–O bond length of HRP compound II at the higher pH might be attributed to the loss of a hydrogen bond which is present between the oxygen ligand and an amino acid residue in the heme pocket at pH 7.

Knowledge of the active-site structure of the heme peroxidases is pivotal to our understanding of the structure ↔ function relationship of this class of enzymes. Horseradish peroxidase (HRP) is perhaps the best characterized heme peroxidase, and its structure has been investigated by numerous techniques (Nozawa et al., 1980; Callahan & Babcock, 1981; deRopp et al., 1984; Penner-Hahn et al., 1983, 1986; Chance et al., 1984). The results of many experiments indicate that the catalytic reaction is centered around the heme. Although an X-ray crystallographic study was recently published (Morita et al., 1991), the resolution is currently insufficient to permit detailed analysis. The amino acid sequence of HRP-C is, however, known (Welinder, 1979) and confirms that the active site is comprised of a heme and a number of amino acid residues, both proximal and distal, which form the heme pocket or cleft. Like most peroxidases, HRP exhibits two catalytically active intermediates—compounds I and II (Yamazaki, 1974). When native HRP reacts with H_2O_2, compound I, which is two oxidizing equivalents above the ferric state, is formed. HRP compound I is subsequently reduced by one electron to form compound II. Reduction of compound II to native enzyme is often rate-limiting in the peroxidase catalytic cycle. The structure of the heme and its immediate environment in compound II is an important aspect of this enzyme mechanism.

Mossbauer (Moss et al., 1969), electron nuclear double resonance (Roberts et al., 1981), NMR (LaMar et al., 1983), X-ray absorption spectroscopy (XAS) (Penner-Hahn et al., 1983, 1986; Chance et al., 1984), and resonance Raman (Hashimoto et al., 1984, 1986a; Terner et al., 1985) studies have shown some double-bond character of the ferryl iron to oxygen bond in compound II of HRP. In addition, Sitter et al. (1985a) and Hashimoto et al. (1986a,b) found that ferryl oxygen is hydrogen-bonded to a distal histidine when the pH is below the pK_a of histidine. Hashimoto et al. (1986a,b) also demonstrated that the oxygen ligand exchanged with oxygen from bulk water. In cytochrome *c* peroxidase, Poulos and Kraut (1980) postulated that distal amino acids are involved in the heterolytic cleavage of H_2O_2 during the formation of compound I (ES). They also showed that distal amino acids are involved in hydrogen bonding to the diatomic ligands (CO, O_2) bound to the heme iron. Yamada and Yamazaki (1975) found similar hydrogen bonding in CN–, CO–, or NO–ligand binding of HRP, as did Asher et al. (1981) with methemoglobin–fluoride complexes. These studies showed that, in addition to peroxide cleavage, there is another role for distal amino acid residues in the stabilization of the sixth ligand of the heme iron. The reaction of HRP compound II is pH dependent since compound II exhibits only weak activity above the pK_a of the distal histidine (Dunford & Stillman, 1976). Changes in the active-site structure of compound II with pH that might explain the altered reactivity may be linked to different geometric relationships with amino acid residues in the heme pocket.

To understand further the reactivity of HRP, it is important to characterize fully the heme structure of compound II. X-ray absorption spectroscopy (XAS) is ideally suited for the investigation of the local environment and electronic structure of the heme iron of heme proteins (Powers, 1982). The extended X-ray absorption fine structure (EXAFS) region contains information about the number and average distance of ligands (±0.015 Å) as well as their relative disorder and provides information on the relative position of the iron atom with respect to the heme plane (Chance et al., 1984, 1986a). The edge region of the spectrum provides information about the valence state of the absorbing atom, the chemical identity of neighboring atoms, and the ligand geometry.

We investigated the active-site structures of HRP compound II using XAS at pH 7 and 10. The results showed significantly different bond distances for the sixth ligand coordinated to the heme iron at the two pH values.

MATERIALS AND METHODS

Sample Preparation. Horseradish peroxidase isoenzyme C (purchased from Toyobo, Osaka, Japan) was dissolved in sodium phosphate buffer (20 mM) for studies at pH 7 and in carbonate buffer (20 mM) for studies at pH 10. By measuring the absorbance at 403 nm (ϵ = 102 mM^{-1} cm^{-1}; Schonbaum & Lo, 1972), we determined the molar concentration of the enzyme at pH 7 and 10. Native HRP reacts with H_2O_2 and ascorbic acid (AH) to produce compound II.

† Supported in part by NIEHS Superfund Grant ES 04922 and by the Savannah River Laboratory, Contract W 89329-BA.

* To whom correspondence should be addressed.
‡ Utah State University.
§ Current address: 7420 Makaska Dr., Derwood, MD 20855.
‖ Brookhaven National Laboratory.

0006-2960/93/0432-923$04.00/0

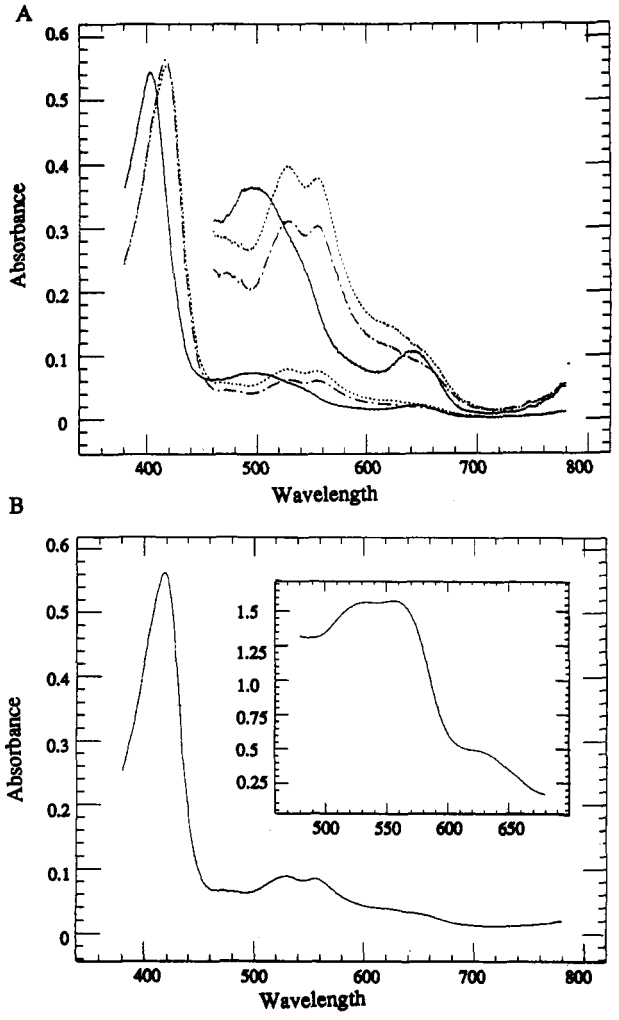

FIGURE 1: (A) Optical spectra of horseradish peroxidase compound II at pH 7 (---) and pH 10 (– • –) and native HRP spectrum at pH 7 (—). The region from 460 to 780 nm is also shown with the absorbance scale multiplied by 5.0. (B) Transmission spectra of XAS sample of HRP compound II at pH 7. Main figure shows transmission spectrum of a diluted aliquot at room temperature. Inset shows transmission spectrum of concentrated sample (~1-mm path length) at ~−100 °C.

The ratio of reactants needed to produce a pure compound II sample varied depending upon the desired final concentration of HRP and the pH. For concentrations less than ~200 μM, the molar ratio HRP:AH:H_2O_2 was 1.0:0.5:1.0 at pH 7 and 10. For the ~2 mM concentration required for XAS studies, we added 40% ethylene glycol and the molar ratio HRP:AH:H_2O_2 was 1.0:0.5:2.2 at pH 7 and 1.0:0.5:3.3 at pH 10.

We used the following technique to obtain efficient mixing. A small aliquot (<10 μL) of H_2O_2 solution was placed at the bottom of a 1.5-mL disposable centrifuge tube and a similar aliquot of an ascorbic acid solution was placed on the wall of the tube so that the two droplets were very close but not touching each other. All components were mixed simultaneously by forcefully pipetting a mixture of HRP, buffer, and ethylene glycol (generally around 150 μL) into the tube. The solution was then drawn back into the pipette and redispensed into the tube. For optical studies, we diluted a small aliquot into buffer solution. The remainder of the solution was immediately loaded into an XAS sample holder and frozen. A control sample of native HRP at pH 7 was also prepared for XAS studies.

We used optical absorption spectroscopy to monitor the conversion of dilute samples (<200 μM) of native enzyme to

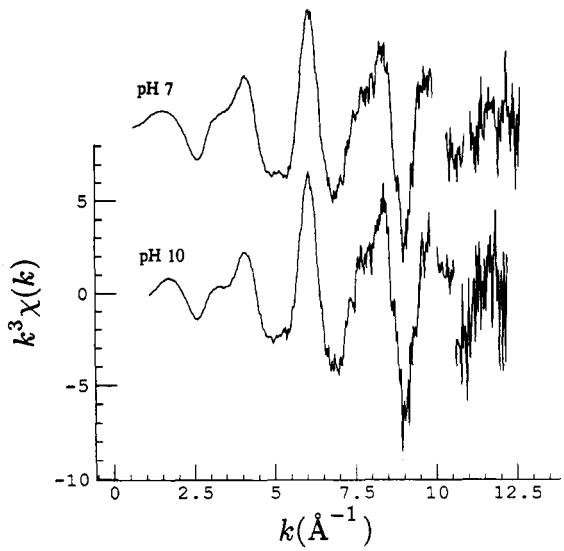

FIGURE 2: (Upper trace) Background-subtracted EXAFS data of HRP compound II at pH 7, normalized to one absorber and multiplied by k^3. (Lower trace) Background-subtracted EXAFS data of HRP compound II at pH 10, normalized to one absorber and multiplied by k^3. The gap in each data set at ~10 $Å^{-1}$ results from the removal of a glitch caused by a higher order reflection of the monochromator crystals.

compound II. For XAS samples (~2 mM), the optical absorption spectra were monitored using either reflectance spectroscopy, transmission spectroscopy of the concentrated material (~1-mm path), or transmission of a diluted aliquot (10-mm path). The spectrum of compound II at pH 10 is almost identical to that at pH 7, with only minor differences (~1 nm) in the position of the Soret band. The purity of HRP compound II was evaluated using a combination of the following criteria: (a) the measured A_{550}/A_{525} ratio following appropriate linear background removal, (b) the minimal value for the 650-nm peak after appropriate linear background removal (Chance, 1952), and (c) for transmission samples only, the position, intensity, and width of the Soret peak. Following X-ray exposure, we recorded transmission spectra of the undiluted length XAS sample (~1-mm path) followed by transmission spectra of a diluted aliquot (10-mm path) (Figure 1B).

Data Collection and Analysis. We recorded XAS data for HRP compound II at both pH values in fluorescence mode at the Stanford Synchrotron Radiation Laboratory (SSRL) Beamline II-2 (Stanford, CA) using a phosphorescent phototube detector (Khalid & Rosenbaum, 1986) as well as at the National Synchrotron Light Source (NSLS) Beamline X9A (Upton, NY) using a 13-element Ge detector system. Both beamline monochromators were equipped with Si(111) crystals providing 2–3-eV resolution at the Fe K-edge. All experiments were carried out at ~155 K to prevent conversion to the native form by hydrated electrons produced from X-ray exposure (Chance et al., 1980).

Following the method of Chance et al. (1984), we calculated the ligand field indicator ratio (LFIR) and analyzed the XAS data using previously described procedures (Powers et al., 1981, 1984; Lee et al., 1981). We analyzed data from each light source separately. Individual scans were summed, followed by background removal of the isolated atoms contribution and multiplication by k^3 (k is the photoelectron wave vector). The final EXAFS modulations shown in Figure 2 were derived by weighted addition of the data from each light source according to their respective signal-to-noise ratios. In both experiments, the data from the two light sources were

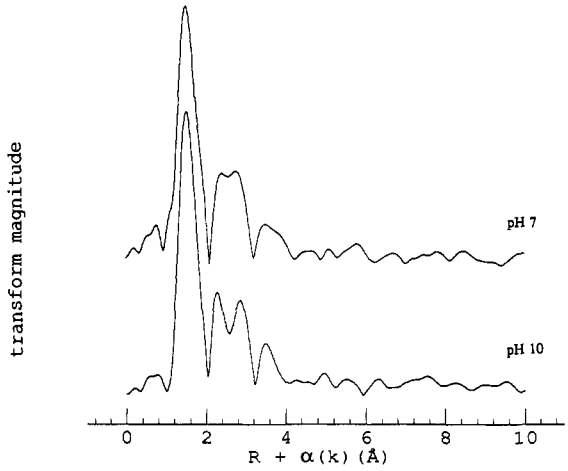

FIGURE 3: Fourier transforms of the EXAFS data of HRP compound II at pH 7 and 10 shown in Figure 2.

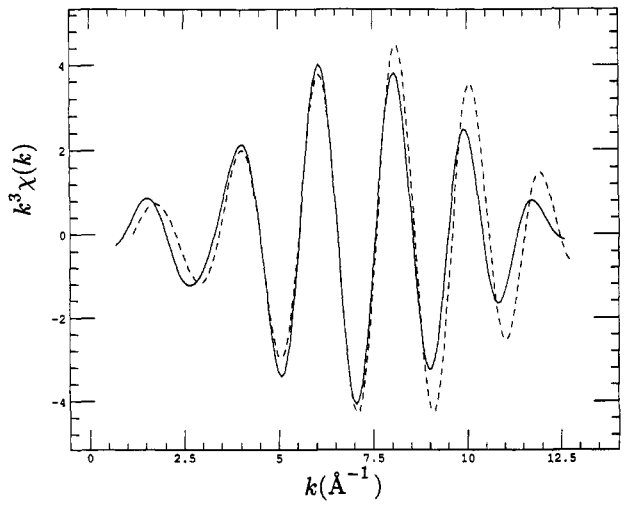

FIGURE 4: Comparison of the first-shell filtered data for HRP compound II at pH 7 (—) and pH 10 (- - -).

identical within the error. The first shell peak of the Fourier-transformed EXAFS modulations (Figure 3) was Fourier filtered and back-transformed (Figure 4). We used these data for fitting procedures.

We collected similar data for three model compounds, bis(imidazole)(tetraphenylporphinato)iron(III) chloride (Collins et al., 1972), (acetylacetonato)iron(II), and (acetylacetonato)-iron(III) (Iball & Morgan, 1967) in transmission mode under identical synchrotron beam conditions. The model compound data were analyzed in the same manner as for the protein samples. Each atom type in the nonlinear fitting procedure is represented by an average distance (r), an amplitude factor containing the number of ligands (N), a change in Debye–Waller factor ($\Delta\sigma^2 = \sigma^2_{model} - \sigma^2_{enzyme}$), and a change in threshold energy ($\Delta E_0 = E_{model} - E_{enzyme}$). To determine possible solutions, we fitted the filtered data for the HRP intermediates with that of the model compounds using a two-atom-type fitting procedure.

Since the number of ligands is highly correlated with $\Delta\sigma^2$, the N parameters were held fixed at their known values (Peisach et al., 1982). Several possible solutions are statistically different only in the $\sum R^2 > \sum R^2_{min}(1 + 1/\phi_f)$ (Powers & Kincaid, 1989). $\sum R^2_{min}$ is the minimum sum of residuals for a physically reasonable solution; the number of independent parameters in the fit, ϕ_f, is equal to $\phi_d - p$, where p is the number of variables in the fit and ϕ_d is the number of degrees of freedom in the filtered data. The variable ϕ_d is estimated to be 8.4 by $2\Delta w\Delta k/\pi$, where Δw is the full width at half-maximum of the filter window (1.1 Å^{-1}) and Δk was the length of the data fit (12 Å^{-1}; Figure 2). Thus the condition is $\sum R^2 > \sum R^2_{min}$ (1.4) for these data. After possible solutions were found for each contribution to the first shell (Fe–N_p, Fe–O, Fe–N_ϵ), we used a three-atom-type consistency test, using all three sets of scatterers with r and N held constant, to verify that the three distances actually coexist in the data (Powers et al., 1984). The $\sum R^2_{min}$ for the three-atom-type consistency test must be smaller than those obtained for the two-atom-type solutions. To ensure that the three distances obtained from the above steps constitute a true minimum, each distance parameter was individually allowed to vary while holding the number parameters and all other distance parameters constant. In each case, the residuals of the consistency test compared favorably to the estimated error over the entire k range.

We determined the total error for each distance by changing a parameter value while holding all other parameters constant, until $\sum R^2$ increased by a factor of 2 on each side of the minimum. Where errors were not symmetric around the minimum, we report the larger value. A detailed discussion of this error analysis is given by Powers and Kincaid (1989).

RESULTS

The preparation of compound II at ~2 mM required higher molar ratios of H_2O_2 to HRP (2.2:1 for pH 7, 3.3:1 for pH 10) than at 200 μM (1:1) as judged by the various criteria discussed in the Materials and Methods section. This behavior is not unique to HRP and has been observed for other peroxidases (Chance et al., 1984). Our determination of the purity of the HRP compound II preparations varied according to the criteria used. Evaluating sample purity using the intensity and position of the Soret band (which is slightly higher in HRP compound II than in native HRP) or using the 530 nm/557 nm absorbance ratio (which is normally 1:1.2 in dilute samples of pure compound II) revealed that our preparations were >90% compound II. Evaluating purity using the intensity of the peak at 650 nm suggested ~80% purity. We prefer the former method as we observe variability of the 650-nm peak with different protein preparations.

Figure 1a shows optical absorption spectra of HRP compound II at pH 7 and 10 and native enzyme at pH 7. There were no apparent spectral changes when the pH of compound II samples increased, except the Soret peak shifted from 417 nm at pH 7 and 418 nm at pH 10. Although we used high concentrations of H_2O_2 in the preparation of compound II, no compound III contamination, which appeared during a study involving myeloperoxidase (Oertling et al., 1988), was apparent in our samples.

The LFIR ratio at both pH values was 1.0 ± 0.05. According to the correlation between LFIR ratio and the iron out-of-plane distance demonstrated by Chance et al. (1986a), the iron of HRP compound II is displaced from the heme plane by ~0.28 ± 0.15 Å at both pH conditions. This is consistent with the average iron-to-pyrrole (Fe–N_p) distances of 2.01 Å. The shape of the LFIR is a consequence of multiple scattering and can also be affected by ruffling of the heme plane.

Table I shows the results of the two-atom-type fitting procedure for compound II at pH 7. The two-atom-type fitting procedure suggests both 1.90 and 2.09 Å as possible axial ligand distances. To confirm these distances, we used a three-atom-type consistency test; the results are shown at the bottom of Table I. Since nitrogen has only one electron fewer than oxygen, EXAFS cannot distinguish between the scattering

Table I: Results of Two-Atom-Type Fitting Procedure and Three-Atom Consistency Test for the First-Coordination Shell of Horseradish Peroxidase Compound II at pH 7

model	N^a	r^b	$\Delta\sigma^{2\,c}$	$\Delta E_0{}^d$	$\sum R^2$
Fe–N	5	2.04	2.7×10^{-3}	–0.4	2.1
Fe–N	1	1.90	5.4×10^{-3}	–3.7	
Fe–N	5	2.00	1.8×10^{-3}	–1.1	2.1
Fe–N	1	2.09	6.5×10^{-3}	2.0	
Fe–N	4	2.01 ± 0.015	2.4×10^{-3}	–0.3	1.9
Fe–N	1	2.09 ± 0.03	4.9×10^{-3}	–0.4	
Fe–N	1	1.90 ± 0.02	4.4×10^{-3}	–4.1	

[a] N, number of ligands, held constant. [b] r, Fe–ligand distance in angstroms. [c] $\Delta\sigma^2$, difference in Debye–Weller factor (model–enzyme) in square angstroms ±45%. [d] ΔE_0, difference in threshold energy (model–enzyme) in electron volts ±2.5 eV.

Table II: Results of Two-Atom-Type Fitting Procedure and Three-Atom Consistency Test for the First-Coordination Shell of Horseradish Peroxidase Compound II at pH 10[a]

model	N	r	$\Delta\sigma^2$	ΔE_0	$\sum R^2$
Fe–N	5	2.01	2.1×10^{-3}	–1.2	1.6
Fe–N	1	1.72	-8.7×10^{-3}	–5.0	
Fe–N	5	2.00	2.1×10^{-3}	–2.3	1.7
Fe–N	1	2.11	-7.6×10^{-3}	5.0	
Fe–N	4	2.00 ± 0.015	3.4×10^{-3}	–0.7	0.7
Fe–N	1	2.11 ± 0.03	-1.1×10^{-3}	–6.8	
Fe–N	1	1.72 ± 0.02	-1.4×10^{-3}	–3.4	

[a] Parameters are defined in Table I.

amplitude of these two atoms, and Fe–N and Fe–O models gave the same results. However, the sixth ligand is probably oxygen, as suggested by the results of Schonbaum and Lo (1972). Therefore, the iron of HRP compound II at pH 7 has four pyrrole nitrogen ligands at an average distance of 2.01 ± 0.015 Å, one axial ligand at 1.90 ± 0.02 Å, and a second axial ligand at 2.09 ± 0.03 Å. No short (1.6–1.7 Å) axial distance was found.

We applied the same fitting procedures described above to data for compound II at pH 10 (Table II) where two-atom-type fitting procedures revealed axial ligand distances of 1.72 and 2.11 Å. When the three-atom-type consistency test was used with these distances, the first coordination shell produced the quantities shown at the bottom of Table II. Thus, the first coordination shell of HRP compound II at pH 10 has four pyrrole nitrogen ligands at an average distance of 2.00 ± 0.015 Å, an axial ligand at 2.11 ± 0.03 Å, and another axial ligand at 1.72 ± 0.02 Å.

In summary, these results show that an axial ligand distance, probably that of the distal oxygen ligand, decreases by ~0.2 Å from pH 7 to 10 while all other ligand distances show no significant change. The higher coordination shells of the Fourier-transformed data reveal differences at the two pH values (Figure 3), indicating movement of nearby amino acid residues and/or deformation of the heme. The data obtained for native HRP at pH 7 were identical to those previously reported (Chance et al., 1984).

DISCUSSION

In these experiments, we used EXAFS spectroscopy to determine the average bond distances of the ligands to the HRP compound II heme iron at pH 7 and 10. At pH 7, the iron is surrounded by four pyrrole nitrogens at an average distance of 2.01 ± 0.015 Å, a fifth ligand at 2.09 ± 0.03 Å, and a sixth ligand at 1.90 ± 0.02 Å. At pH 10, the results indicate four pyrrole nitrogens at an average distance of 2.00 ± 0.015 Å, a fifth ligand at 2.11 ± 0.03 Å, and a sixth ligand

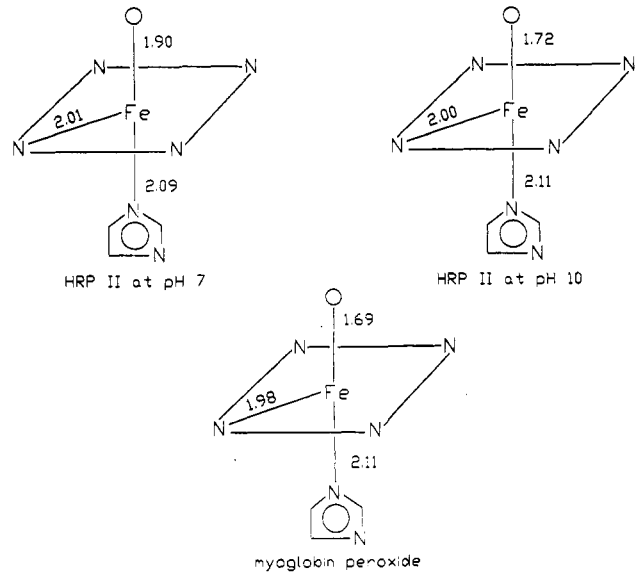

FIGURE 5: Active-site structures of HRP compound II at pH 7 and 10 compared with the active site structure of myoglobin peroxide. Distances are in angstroms, and errors are given in the text.

at 1.72 ± 0.02 Å. Only the sixth ligand bond distance decreased by ~0.2 Å at pH 10 from that at pH 7. These results are summarized in Figure 5 and are consistent with the results of other peroxidases which have been summarized and compared with globins by Chance et al. (1984).

The results at pH 7 reported here agree with the active-site structure of HRP compound II, also at pH 7, reported by Chance et al. (1984). Like Chance et al., we could not distinguish the difference between nitrogen and oxygen in the sixth position. A distance of 2.09 Å for an oxygen ligated to a low-spin heme iron is physically less reasonable than 1.89 Å. Therefore, 2.09 Å is favored for the proximal ligand distance and 1.89 Å is assigned to the Fe–O bond length. With hydrogen bonding between a distal base and the sixth ligand at pH 7, the Fe–O bond will elongate as electrons in the bond are pulled toward the distal amino acid. This redistribution of electrons might explain the increased reactivity of HRP compound II at pH 7 since it would allow the intermediate to be readily reduced by a second substrate (Dunford & Stillman, 1976; Hayashi & Yamazaki, 1979; Nakajima & Yamazaki, 1987).

Penner-Hahn et al. (1983, 1986) reported structures for HRP compounds I and II with short axial ligand distances. Chance et al. (1984) agree with Penner-Hahn et al. (1983) that compound I contains a short axial ligand distance. Our results disagree with Penner-Hahn (1986) and agree with Chance et al. (1984) that no short axial ligand is found at pH 7 for compound II. However, we observed a short axial distance at pH 10. Clearly, the data reported in these studies are different, and the different results cannot be attributed to the analysis procedures, which are similar (Penner-Hahn et al., 1986; Chance et al., 1984).

Over the past few years, we have collected data on HRP compound II samples that were isolated and characterized in several different laboratories. These samples were all ~2 mM (pH 7) and contained ~40% ethylene glycol, and the data were collected at temperatures ≤155 K on various beamlines at both the Stanford Synchrotron Radiation Laboratory and the National Synchrotron Light Source. In every case, the integrity and purity of the compound II sample was assessed by the methods described in the Materials and Methods section using both transmission and reflectance

optical spectroscopy. These data and results were all identical to each other and to those reported by Chance et al. (1984). Therefore, other explanations for the differences reported by Penner-Hahn et al. (1983, 1986) must be considered.

There are three major differences in sample preparation and data collection between methods in this paper and by Chance et al. (1984) and those reported by Penner-Hahn et al. (1983, 1986): (1) Samples of Penner-Hahn et al. did not contain ~40% ethylene glycol. (2) Samples of Penner-Hahn et al. were more than twice as concentrated as those reported here and were produced by different methods. (3) The temperature of the sample during data collection reported by Penner-Hahn et al. was ~60 K higher than that reported here.

In order to explain these differences, we consider the following possibilities: (1) Ethylene glycol affects the conversion to compound II. Compound I production is apparently not affected by using ethylene glycol because the results of Chance et al. (1984) agree with those of Penner-Hahn et al. (1983). We attempted to explore this possibility by preparing compound II without ethylene glycol. Although we were able to produce highly concentrated samples for XAS studies, the data consistently contained artifacts (Chance et al., 1983, 1984), probably due to diffraction from ice crystals. Our samples required the addition of at least 30% ethylene glycol to collect artifact-free data.

(2) The mixing of 1 equiv of ascorbic acid with the highly concentrated (7.5 mM) compound I by Penner-Hahn et al. (1986) was insufficient to convert the sample to compound I (except possibly at the interfaces between the compound I preparation and the added ascorbate where the sample was adequately mixed). Our experience has shown that efficient mixing is especially difficult with small volumes (<200 μL) of highly concentrated viscous samples, particularly in XAS sample holders. However, even in an insufficiently mixed sample, it is likely that mixing, and thus conversion, proceeds to completion when the material is diluted for optical studies. This possibility is difficult to assess, since no optical data were given by Penner-Hahn et al. (1986) for the highly concentrated samples used in their studies.

(3) Hashimoto et al. (1986a,b) showed that the oxygen ligand of compound II can rapidly exchange with the oxygen of water at pH 7 but not at pH 11. They propose a mechanism for this exchange where the heme-bound oxygen and a proton of a distal amino acid combine as OH^- and exchange with bulk water. XAS results would then give an average of the structures present during this exchange. However, it is likely that this exchange equilibrium is not only temperature dependent but also sensitive to the method of freezing (i.e., the presence or absence of ethylene glycol and rate of freezing). In this case, XAS results would not give an average of the various structures present during this rapid exchange but, rather, an average of the structures present as influenced by the freezing process. This could also explain why our result of 1.90 Å for the Fe–O bond distance is longer than that expected for an Fe–O bond with some double-bond character at ambient temperatures (Hashimoto et al., 1984; Terner et al., 1985). It is important to note that the observed resonance Raman frequencies for compound II are 40–80 cm^{-1} lower than those for Fe^{IV}=O model compounds (Schappacher et al., 1986; Bajdor & Nakamoto, 1984).

Badger's rule, an empirical rule developed for diatomic molecules, may not hold for the molecules under consideration here. Badger's rule predicts a change of ~0.01 Å for a 10-cm^{-1} decrease. The change difference of 0.18 Å between the Fe–O bond length at pH 7 and 10 we find is larger than that predicted by Badger's rule for the change in observed Raman frequencies (8–17 cm^{-1}) (Hashimoto et al., 1984; Terner et al., 1985; Makino et al., 1986). However, similar results were also reported by Walters et al. (1980) for Fe^{+2}(TpivPP)(2-MeIm)-O_2 and Fe^{+2}(TpivPP)(1-MeIm)O_2 [TpivPP = 5,10,15,20-($\alpha,\alpha,\alpha,\alpha$)-(*o*-pivaloylamidophenyl)porphyrinate]. Walters et al. (1980) pointed out that an 8–11-cm^{-1} decrease is much too small for the Fe–O bond distance change of 0.15 Å found by crystallography studies (Jameson et al., 1978, 1980). XAS results of these oxygen adducts (Woolery et al., 1985) obtained under conditions similar to those reported here, agree with the crystallography results.

Although our results are not in quantitative agreement with the various resonance Raman studies, they are in good qualitative agreement. Both XAS and resonance Raman studies clearly indicate a shorter Fe–O distance at high pH where there is no distal hydrogen bond (Sitter et al. 1985a; Hashimoto et al., 1986a). All resonance Raman high frequencies (>1000 cm^{-1}) and most low frequencies of compound II are unchanged at pH 7 and 10, in agreement with our results. In our experiment, the average Fe–N_p distance and Fe–proximal ligand distance are unchanged within the error, as are the LFIR ratios. Since the optical spectrum results largely from $\pi \rightarrow \pi^*$ transitions in the porphyrin (Gouterman, 1959), our results also explain the similarity of the optical absorption spectra of HRP compound II at pH 7 and 10 (Figure 1a). Similarly, Sitter et al. (1985b) compare resonance Raman results for compound II and myoglobin peroxide (ferryl myoglobin). HRP compound II at pH 7 differs mainly in the Fe–O stretching frequency and has a somewhat larger core size than myoglobin peroxide. At pH 10, however, the Fe–O stretching frequency of HRP compound II approaches that of myoglobin peroxide. Results of XAS studies of myoglobin peroxide (Chance et al. 1986b), obtained under similar conditions to those for HRP reported from our experiments, agree with both these conclusions. The Fe–O distance for myoglobin peroxide (1.69 ± 0.03 Å) and that for compound II at pH 10 (1.72 ± 0.02 Å) are identical within the error, while the Fe–N_p average distance is 1.98 ± 0.02 Å for myoglobin peroxide and that for compound II at pH 10 is 2.00 ± 0.015 Å.

The outer shells observed by XAS in heme proteins and model compounds are due largely to the heme with some contributions from the proximal histidine. The heme porphyrin is a relatively rigid structure which changes little, if at all, with pH changes since the average Fe–N_p distances are identical. Nevertheless, there are differences for the higher shells. In view of these results as well as other studies, it is difficult to attribute these differences to heme contributions alone. It is unlikely that these differences are due to differences in resolution of the data since the data at both pH values were collected at the same time under identical conditions. One explanation might be the movement of an amino acid residue within a 3–4-Å radius of the iron. It is widely accepted that, in peroxidases, amino acid residues around the active site stabilize the oxidized state of the iron center during the catalytic reaction. Yamazaki et al. (1978), Poulos and Kraut (1980), and Poulos and Finzel (1984) suggested that amino acid residues, such as histidine, arginine, and tryptophan, that are distal to the heme of various peroxidases can interact strongly with the sixth ligand of the heme iron during normal activity. These results are consistent with the model proposed by Ator et al. (1987) in which spatial rearrangement of amino acid residues distal to the heme controls the heme reactivity.

Using resonance Raman spectroscopy, Hashimoto et al. (1986b) propose that a hydrogen-bonded protein from a distal amino acid is essential to acid–base catalysis in HRP. They attribute the alkaline inactivation of HRP to disruption of this hydrogen bond at high pH. Our results are entirely consistent with the mechanism they propose (Hashimoto et al., 1986a, Figure 5). At pH 7, the distal hydrogen bonding elongates the Fe=O bond, while at pH 9, the absence of the distal hydrogen allows the Fe=O bond to relax to a shorter distance (Hashimoto et al., 1986a, Figure 5d,e). A change in Fe–O distance of 0.2 Å in response to the hydrogen-bonding differences is very reasonable and could easily explain the pH-dependent differences in reactivity.

In summary, XAS results at <155 K show that the Fe–O bond distance at compound II decreases by ~0.18 Å from pH 7, where the oxygen ligand is hydrogen-bonded to an amino acid in the distal pocket, to pH 10, where this hydrogen bond is absent. However, both the Fe–N_ϵ and average Fe–N_p distances remain unchanged. For compound II at pH 10, these distances are similar to those for myoglobin peroxide. Changes in the higher coordination shells might be attributed to movement of residues in the distal pocket.

ACKNOWLEDGMENT

We thank the National Biostructures Participating Research Team for allocation of beam time and experimental support on X-9 at the National Synchrotron Light Source, Brookhaven National Laboratory, Upton, Long Island, NY. The Biostructures PRT (Beamline X9A, NSLS/BNL) is supported by NIH RR-01633. The SSRL Biotechnology Program is supported by the NIH, Biomedical Resource Technology Program, Division of Research Resources.

REFERENCES

Asher, S. A., Adams, M. L., & Schuster, T. M. (1981) *Biochemistry 20*, 3339–3346.
Ator, M. A., & Ortiz de Montellano, P. R. (1987) *J. Biol. Chem. 262*, 1542–1551.
Bajdor, K., & Nakamoto, K. (1984) *J. Am. Chem. Soc. 106*, 3045–3046.
Callahan, P., & Babcock, G. (1981) *Biochemistry 20*, 952–958.
Chance, B. (1952) *Arch. Biochem. Biophys. 41*, 416–424.
Chance, B., Angiolillo, P., Yang, E., & Powers, L. (1980) *FEBS Lett. 112*, 178–180.
Chance, B., Fischetti, R., & Powers, L. (1983) *Biochemistry 22*, 3820–3829.
Chance, B., Powers, L., Ching, Y., Poulos, T. L., Schonbaum, G. R., Yamazaki, I., & Paul, K. G. (1984) *Arch. Biochem. Biophys. 235*, 596–611.
Chance, M., Parkhurst, L., Powers, L., & Chance, B. (1986a) *J. Biol. Chem. 261*, 5689–5692.
Chance, M., Powers, L., Kumar, C., & Chance, B. (1986b) *Biochemistry 25*, 1259–1265.
Collins, D., Countryman, R., & Hoard, J. (1972) *J. Am. Chem. Soc. 94*, 2066–2072.
de Ropp, J. S., La Mar, G. N., Smith, K. M., & Langry, K. C. (1984) *J. Am. Chem. Soc. 106*, 4438–4444.
Dunford, H. B., & Stillman, J. S. (1976) *Coord. Chem. Rev. 19*, 187–251.
Gouterman, M. (1959) *J. Chem. Phys. 30*, 1139–1161.
Hashimoto, S., Tatsuno, Y., & Kitagawa, T. (1984) *Proc. Jpn. Acad. Ser. B60*, 345–348.
Hashimoto, S., Tatsuno, Y., & Kitagawa, T. (1986a) *Proc. Natl. Acad. Sci. U.S.A. 83*, 2417–2421.
Hashimoto, S., Nakajama, R., Yamazaki, I., Tatsuno, Y., & Kitagawa, T. (1986b) *FEBS Lett. 208*, 305–307.
Hayashi, Y., & Yamazaki, I. (1979) *J. Biol. Chem. 254*, 9101–9106.
Iball, J., & Morgan, C. (1967) *Acta Crystallogr. 23*, 239–244.
Jameson, G., Molinaro, F., Ibers, J., Collman, J., Brauman, J., Rose, E., & Suslick, K. (1978) *J. Am. Chem. Soc. 100*, 6769–6770.
Jameson, G., Molinaro, F., Ibers, J., Collman, J., Brauman, J., Rose, E., & Suslick, K. (1980) *J. Am. Chem. Soc. 102*, 3224–3237.
Khalid, S., & Rosenbaum, G. (1986) *Proc. SPIE—Int. Soc. Opt. Eng. 690*, 65–67.
La Mar, G. N., de Ropp, J. S., Latos-Grazynski, L., Balch, A. L., Johnson, R. B., Smith, K. M., Parish, D. W., & Cheng, R.-J. (1983) *J. Am. Chem. Soc. 105*, 782–787.
Lee, P. A., Citrin, P. H., Eisenberger, P., & Kincaid, B. M. (1981) *Rev. Mod. Phys. 53*, 769–806.
Makino, R., Uno, T., Nishimura, Y., Iizuka, T., Tsuboi, M., & Ishimura, Y. (1986) *J. Biol. Chem. 261*, 8376–8382.
Morita, Y., Mikami, B., Yamashita, H., Lee, J. Y., Aibara, S., Sata, M., Katsube, Y., & Tanaka, N. (1991) in *Biochemical, Molecular, and Physiological Aspects of Plant Peroxidases* (Labarzewski, J., Greppin, H., Panel, C., & Gaspar, Th., Eds.), pp 81–88, University of Geneva, Geneva, Switzerland.
Moss, T. H., Ehrenberg, A., & Bearden, A. J. (1969) *Biochemistry 8*, 4159–4162.
Nakajima, R., & Yamazaki, I. (1987) *J. Biol. Chem. 262*, 2576–2581.
Nozawa, T., Kobayashi, N., Hatano, M., Veda, M., & Sagan, M. (1980) *Biochim. Biophys. Acta 626*, 282–290.
Oertling, W., Hoogland, H., Babcock, G., & Wever, R. (1988) *Biochemistry 27*, 5395–5400.
Peisach, L., Powers, L., Blumberg, W. E., & Chance, B. (1982) *Biophys. J. 38*, 227–285.
Penner-Hahn, J. E., McMurry, T. J., Renner, M., Latos-Grazynski, L., Eble, K. S., Davis, I. M., Balch, A. L., Groves, J. T., Dawson, J. H., & Hodgson, K. O. (1983) *J. Biol. Chem. 258*, 12761–12764.
Penner-Hahn, J. E., Eble, K. S., McMurry, T. J., Renner, M., Balch, A. L., Groves, J. T., Dawson, J. H., & Hodgson, K. O. (1986) *J. Am. Chem. Soc. 108*, 7819–7825.
Poulos, T. L., & Kraut, J. (1980) *J. Biol. Chem. 255*, 8199–8205.
Poulos, T. L., & Finzel, B. C. (1984) *Pept. Protein Rev. 4*, 115–171.
Powers, L. (1982) *Biochim. Biophys. Acta 683*, 1–38.
Powers, L., & Kincaid, M. (1989) *Biochemistry 28*, 4461–4468.
Powers, L., Chance, B., Ching, Y., & Angiolillo, P. (1981) *Biophys. J. 34*, 465–498.
Powers, L., Sessler, J. L., Woolery, G. L., & Chance, B. (1984) *Biochemistry 23*, 5519–5523.
Roberts, J. E., Hoffman, B. M., Rutter, R., & Hager, L. P. (1981) *J. Am. Chem. Soc. 103*, 7654–7655.
Schappacher, M., Chattard, G., & Weiss, R. (1986) *J. Chem. Soc., Chem. Commun.*, 93–94.
Schonbaum, G. R., & Lo, S. (1972) *J. Biol. Chem. 247*, 3353–3360.
Sitter, A. J., Reczek, C. M., & Terner, J. (1985a) *J. Biol. Chem. 260*, 7515–7522.
Sitter, A. J., Reczek, C. M., & Terner, J. (1985b) *Biochim. Biophys. Acta 828*, 229–235.
Terner, J., Sitter, A. J., & Reczek, C. M. (1985) *Biochim. Biophys. Acta 828*, 73–80.
Walters, M. A., Spiro, T. G., Suslick, K., & Collman, J. (1980) *J. Am. Chem. Soc. 102*, 6857–6858.
Welinder, K. G. (1979) *Eur. J. Biochem. 96*, 483–502.
Woolery, G., Walters, M., Suslick, K., Powers, L., & Spiro, T. (1985) *J. Am. Chem. Soc. 107*, 2370–2373.
Yamada, H., & Yamazaki, I. (1975) *Arch. Biochem. Biophys. 171*, 737–744.
Yamazaki, I. (1974) in *Molecular Mechanisms of Oxygen Activation* (Hayaishi, O., Ed.) pp 535–448, Academic Press, New York.
Yamazaki, I., Araiso, T., Hayashi, Y., Yamada, H., & Makino, R. (1978) *Adv. Biophys. 11*, 249–281.